

## Effect of layer-thickness fluctuations on superlattice diffraction

B. M. Clemens and J. G. Gay

*Physics Department, General Motors Research Laboratories, Warren, Michigan 48090-9055*

(Received 19 December 1986)

We investigate the effect of layer-thickness fluctuations on diffraction in compositionally modulated materials. Two types of fluctuation distributions are considered: continuous random fluctuations which result from disordered or amorphous interfaces and discrete fluctuations resulting from coherent interfaces. We show that these two types of fluctuations produce identical superlattice diffraction structure at small scattering vector, but entirely different structure at large scattering vector corresponding to the discrete fluctuation spacing. Both structures are observed in experimental x-ray diffraction spectra.

There is much interest in the structure of superlattices and compositionally modulated materials formed by imposing an atomic-scale artificial periodicity during growth of a film.<sup>1</sup> The structure of these materials covers the entire spectrum from single crystals to completely amorphous materials depending on growth conditions and the size and structure mismatch of the constituents.

The diffraction pattern of a perfect superlattice with a precise composition-modulation wavelength may have superlattice peaks in the growth direction at any scattering vector  $Q$  that is a multiple of  $2\pi$  over the wavelength. Whenever a real superlattice possesses strong composition modulation and a well-defined average composition-modulation wavelength, its x-ray diffraction pattern exhibits these superlattice peaks at small scattering vector  $Q$ . However, at large scattering vector two qualitatively different behaviors may occur. In one case, which is usually observed when there is structural size mismatch of 10% or less, the superlattice peaks reappear in the vicinity of the  $Q$  corresponding to a plane spacing in the growth direction. These features have even been seen in cases where there is a symmetry mismatch between mating planes, such as in Nb-Cu (Refs. 2 and 3) and Mo-Ni (Ref. 4). An example is shown in Fig. 1(a), which is the diffraction pattern in the growth direction for a Mo-Ni multilayer with a composition-modulation wavelength of 8 nm prepared by sputter deposition.<sup>5</sup> The data are plotted versus the scattering angle  $2\theta$  which is related to the scattering vector  $Q$  by  $Q = 4\pi \sin(\theta)/\lambda$ , where  $\lambda = 0.154$  nm is the x-ray wavelength.

In the other case, which tends to occur with more severe structural size mismatch ( $>15\%$ ), no superlattice peaks appear at large  $Q$ . This is illustrated in Fig. 1(b) which shows the diffraction pattern from a Ni-Ti multilayer structure with a composition-modulation wavelength of 8 nm prepared in exactly the same manner.<sup>5</sup> The broad maxima observed in the high-angle (large- $Q$ ) region are associated with scattering from individual Ti and Ni layers. This system nevertheless shows sharp superlattice peaks at small  $Q$  indicating strong composition modulation. This type of diffraction result is typical of systems with large structural mismatch between the constituents, such as Ti-Ni,<sup>5</sup> Cu-Hf,<sup>6</sup> and Ni-Zr,<sup>5</sup> or in cases where one constituent is amorphous or disordered such as Nb-Ge

(Ref. 7) or Co-Sb.<sup>8</sup> Nakayama *et al.*,<sup>8</sup> and more recently Sevenhans *et al.*<sup>9</sup> have demonstrated that fluctuations of 0.1 nm in the spacing between the slabs of the crystalline component will result in this effect. Layer-thickness fluctuations of 0.1 nm are impossible to avoid in preparation of multilayer samples, and one is left with the question of why superlattice lines are *ever* observed in the high-angle region.

The nature of the interface is central to this issue. In cases where high-angle superlattice lines are observed, the lattice mismatch between the constituents is small and interfaces are coherent. Even in cases where there is a symmetry difference in the mating planes, such as exists be-

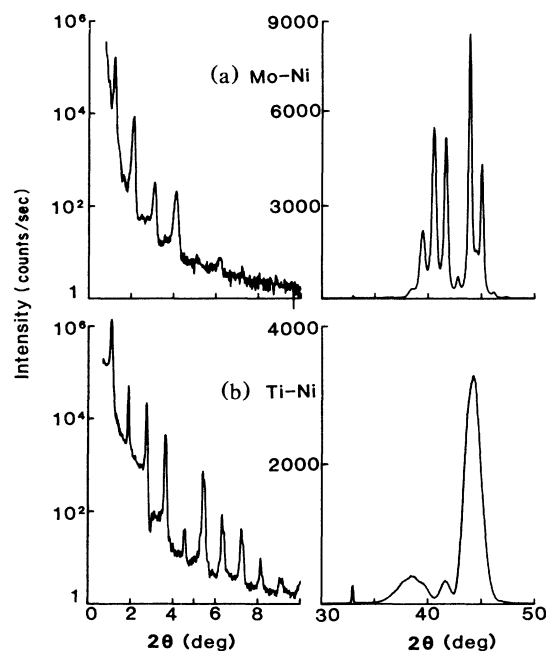


FIG. 1. X-ray diffraction pattern for compositionally modulated films with a composition modulation-wavelength of 8 nm. Shown are both low- and high-angle regions. (a) is Mo-Ni and (b) is Ti-Ni. Both films were prepared by sputter deposition in exactly the same manner.

tween the Ni (111) and Mo (110) planes, registry is possible due to a matching of the spacing between rows of atoms.<sup>10</sup> Crystalline coherency across an interface confines fluctuations in layer thickness to be multiples of the plane spacing of either constituent (or even some average plane spacing in the case where there is some alloying). However, in the presence of an amorphous phase there can be a continuous distribution of layer thickness. The amorphous phase can arise either from the structure of one of the constituents or due to interfacial disorder (as is seen in systems where the constituents are crystalline but there is a large size mismatch<sup>5,6</sup>).

In this Communication we present for the first time analytical diffraction patterns for superlattices with discrete layer-thickness fluctuations. These were obtained using a generalized-Patterson-function approach which can also give the diffraction when the layer fluctuations are continuous. In addition, we have performed numerical simulations of diffraction from multilayers constructed with either type of fluctuation. Both approaches yield similar results and show that the large- $Q$  superlattice structure only appears when the fluctuations are discrete.

The electron density of a superlattice layered in the  $z$  direction is the convolution of the electron density of a single layer with the distribution function of the layers  $h(z)$ .<sup>11</sup> Consequently, when the scattering vector  $Q$  is along  $z$ , the scattering amplitude is the product of the layer structure factor,  $S(Q)$ , and the Fourier transform,  $D(Q)$  of the layer distribution function.<sup>11</sup> The scattering intensity is therefore

$$|F(Q)|^2 = |S(Q)|^2 |D(Q)|^2, \quad (1)$$

$$G_n(z) = \mathcal{N}_n \sum_{m=-\infty}^{\infty} \delta(z - nc - md) [\delta(z - nc) * \exp(-z^2/|n|\sigma^2)], \quad (5)$$

where  $\mathcal{N}_n$  is a factor which normalizes the probability distribution. In Eq. (5), the convolution inside the brackets is to be done before multiplication by the left  $\delta$  function. The Fourier transform of this generalized Patterson function is

$$|D(Q)|^2 = N + 2 \sum_{n=1}^{N-1} \mathcal{N}_n (N-n) \cos(ncQ) \left[ 1 + 2 \sum_{m=1}^{\infty} \exp(-m^2 d^2/n\sigma^2) \cos(mdQ) \right]. \quad (6)$$

For small  $Q$  the transforms (4) and (6) differ only by terms of order  $Q^2$ . Both have a maximum of  $N^2$  at  $Q=0$  with additional superlattice maxima when  $Q$  is a multiple of  $\pm 2\pi/c$ , all of which diminish with  $|Q|$  at a rate which depends on  $\sigma$ . For  $|Q|$  large compared to  $1/\sigma$ , (4) damps to a constant value of  $N$ , whereas (6) contains images of the small- $Q$  superlattice structure centered about values of  $Q$  which are a multiple of  $\pm 2\pi/d$ . If  $c$  is a multiple of  $d$ , (6), is, in fact, periodic in  $Q$  with period  $2\pi/d$ .

In Fig. 2 we show the high- $Q$  behavior of the scattering intensity  $|F(Q)|^2$  and its two factors  $|D(Q)|^2$  and  $|S(Q)|^2$  for a superlattice composed of 10 layers each consisting of 20 atomic planes of Ni(111) plus a non-scattering component with an average thickness equal to 20 atomic planes of Ti(002). The Ti (002)  $d$  spacing was used for the discrete fluctuation spacing  $d$ , and also for the distribution half-width  $\sigma$ . Solid lines are used for the discrete case and dashed for continuous. The Fourier transform of the generalized Patterson function in Fig. 2(a) shows the behavior described above. Scattering in-

where  $|D(Q)|^2$  is the Fourier transform of the generalized Patterson function  $h(z)*h(-z)$ , the self-convolution of the layer distribution function.<sup>11</sup>

Consider a superlattice in which the repeating layers have identical electron distributions but in which the spacing between adjacent layers has a Gaussian distribution of half-width  $\sigma$  about the average spacing  $c$ . The  $n$ th-neighbor distribution is an  $n$ -fold convolution of the first-neighbor distribution.<sup>11</sup> Thus an  $N$ -layer superlattice will have the generalized Patterson function

$$h(z)*h(-z) = \sum_{n=-N+1}^{N-1} (N-|n|)G_n(z), \quad (2)$$

where

$$G_n(z) = \delta(z - nc) * \frac{\exp(-z^2/|n|\sigma^2)}{\sqrt{\pi|n|\sigma^2}}. \quad (3)$$

This generalized Patterson function reduces in the limit of large  $N$  to the expression for an infinite superlattice given on page 153 of Ref. 11. Its Fourier transform is<sup>9</sup>

$$|D(Q)|^2 = N + 2 \sum_{n=1}^{N-1} (N-n) \cos(ncQ) \exp(-n\sigma^2 Q^2/4). \quad (4)$$

Consider now a different superlattice in which the first-neighbor spacing is not continuously distributed about the average, but in which the spacing differs from  $c$  by  $md$ , where  $m$  is an integer and  $d$  is some plane spacing of the layer. If the probability that the spacing is  $c + md$  is proportional to  $\exp(-m^2 d^2/\sigma^2)$ , the generalized Patterson function is Eq. (2) with

tensities are shown in Fig. 2(c). Since the continuous Fourier transform of the generalized Patterson function is structureless, the scattering intensity for the continuous case is just the square of the structure factor for the individual nickel layers [Fig. 2(b)]. On the other hand, the scattering intensity for the discrete case shows superlattice peaks because the Ni structure factors overlap the superlattice structure image in the Fourier transform of the generalized Patterson transform. This occurs because the Ni (111)  $d$  and Ti (002)  $d$  spacings are sufficiently close. The decay of this discrete transform away from the scattering angle corresponding to the Ti (002)  $d$  spacing will become more pronounced as  $\sigma$  is increased. In a more realistic calculation, the thickness of the Ni layers will also fluctuate, with  $d$  equal to the Ni (111)  $d$  spacing. The Fourier transform of the generalized Patterson function and thus the scattering intensity may then have superlattice peaks in the regions corresponding to both the Ti (002) and the Ni (111)  $d$  spacings.

As a check on the above analysis, numerical simula-

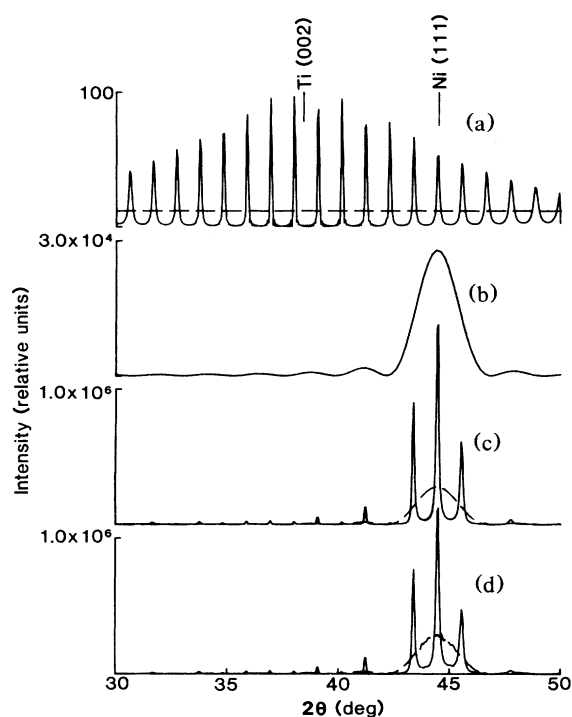


FIG. 2. Theoretical results for diffraction quantities described in the text for a superlattice comprised of 10 layers of 20 Ni (111) atomic planes separated by a nonscattering layer of average thickness equal to 20 Ti (002) atomic planes. The dashed line is for a continuous layer thickness fluctuation distribution. The solid line is for a discrete fluctuation distribution with the spacing equal to the Ti (002)  $d$  spacing. In both, the half width of the distribution is equal to the Ti (002)  $d$  spacing. (a) is the Fourier transform of the generalized Patterson function, (b) is the square of the structure factor for a single layer of Ni (111) planes, (c) is the diffraction intensity, (d) is the diffraction intensity calculated by numerical simulation as described in the text.

tions were performed using one-dimensional kinematic diffraction theory which predicts the diffracted intensity

$$|F(Q)|^2 = \left| \sum_{n=1}^{N_p} f_n(Q) \exp(iQz_n) \right|^2, \quad (7)$$

where  $f_n(Q)$  is the scattering factor of the atoms of the  $n$ th atomic plane,  $z_n$  is the position of this plane, and  $N_p$  is the total number of atomic planes in the structure. We simulated exactly the Ni/Ti superlattices modeled with the generalized-Patterson-function approach. There were 10 layers with each layer consisting of 20 scattering Ni (111) planes and 20 nonscattering Ti (002) planes. Thus,  $N_p = 400$ . The thickness of the Ti in a given layer was sampled from a Gaussian distribution of half-width  $\sigma$  equal to the Ti (002)  $d$  spacing. The thicknesses were allowed to remain continuous or were made discrete by rounding to the nearest multiple of the Ti (002)  $d$  spacing.

In a real superlattice, the thickness of each layer will fluctuate as a function of position within the layer, and since the lateral coherence of the x-ray beam is about 10

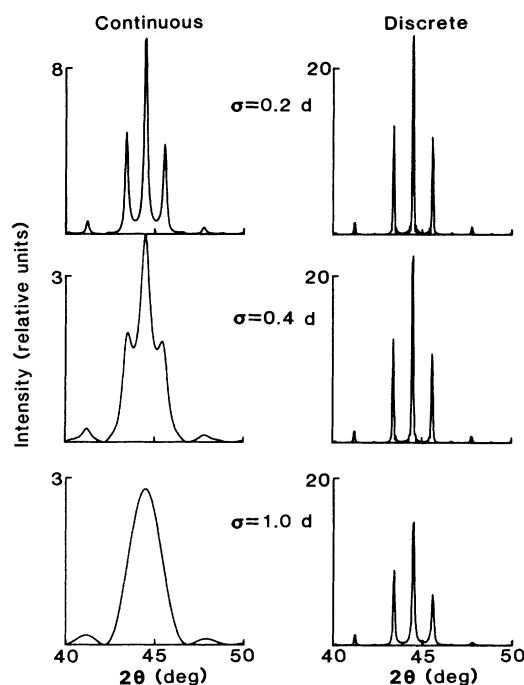


FIG. 3. Diffraction intensity calculated by the Patterson approach for superlattice structures as described in the text for several layer thickness fluctuation distribution half widths. Results are shown for both continuous and discrete fluctuation distributions.  $d$  is the Ti (002)  $d$  spacing.

nm, the actual experiment is an averaging of many distinct superlattice structures. To simulate this effect, we averaged over 500 examples of superlattices constructed as described above. The results for both random and discrete fluctuations are shown in Fig. 2(d) and are virtually indistinguishable from those calculated by the generalized-Patterson-function method. We regard this as convincing evidence that this method is correct and, in particular, that the  $n$ th neighbor spacing is an  $n$ -fold convolution.<sup>11</sup>

A comparison of the effect of  $\sigma$  on random and discrete high-angle fluctuation spectra is shown in Fig. 3. The superlattice peaks are quickly washed out in the case of continuous fluctuations, and disappear by the time  $\sigma$  is equal to the Ti (002)  $d$  spacing. On the other hand, for discrete fluctuations there is only a slight reduction in intensity and a washing out of the ringing between the superlattice peaks. Since higher-order diffraction maxima are not decreased in intensity by discrete fluctuations, care must be taken when using peak intensity ratios as a diagnostic for layer-thickness uniformity.

In summary, the occurrence of superlattice peaks at  $Q = 2\pi/d$ , where  $d$  is an atomic plane spacing, is dependent on the nature of the layer thickness fluctuations. A continuous layer thickness distribution will wash out superlattice lines in this region at very small values of  $\sigma$ . If, on the other hand, the layer thickness distribution is discrete, we have shown that the superlattice lines will survive for values of  $\sigma$  that are easily realized experimentally.

- <sup>1</sup>See, for example, *Synthetic Modulated Structures*, edited by L. L. Chang and B. C. Giessen (Academic, New York, 1985).
- <sup>2</sup>I. K. Schuller, *Phys. Rev. Lett.* **44**, 1597 (1980).
- <sup>3</sup>W. P. Lowe, T. W. Barbee, T. H. Geballe, and D. B. McWhan, *Phys. Rev. B* **24**, 6193 (1981).
- <sup>4</sup>M. R. Kahn, C. S. L. Chun, G. P. Felcher, M. Grimsditch, A. Kueny, C. M. Falco, and I. K. Schuller, *Phys. Rev. Lett.* **27**, 7186 (1983).
- <sup>5</sup>B. M. Clemens, *Phys. Rev. B* **33**, 7615 (1986).
- <sup>6</sup>S. M. Heald, J. M. Tranquada, B. M. Clemens, and J. P. Stec, *J. Phys.* (Paris) (to be published).
- <sup>7</sup>S. T. Ruggiero, T. W. Barbee, and M. R. Beasley, *Phys. Rev. B* **26**, 4894 (1982).
- <sup>8</sup>N. Nakayama, K. Takahashi, T. Shinjo, T. Takada, and H. Ichinose, *Jpn. J. Appl. Phys.* **25**, 552 (1986).
- <sup>9</sup>W. Sevenhans, M. Gijs, Y. Bruynseraede, H. Homma, and I. K. Schuller, *Phys. Rev. B* **34**, 5955 (1986).
- <sup>10</sup>E. Bauer and J. H. van der Merwe, *Phys. Rev. B* **33**, 3657 (1986).
- <sup>11</sup>J. M. Cowley, *Diffraction Physics* (North-Holland, Amsterdam, 1981).